Quantum interference effects in a Pi -shaped electron waveguide

1993 Semicond. Sci. Technol. 8 2115

(http://iopscience.iop.org/0268-1242/8/12/014)

Semicond. Sci. Technol. 8 (1993) 2115–2120. Printed in the UK

Quantum interference effects in a Π-shaped electron waveguide

A I Onipko† and I V Zozulenko†‡

† Bogolyubov Institute for Theoretical Physics, Academy of Sciences of Ukraine, Kiev, 252143, Ukraine
†‡ Division of Physics, The Norwegian Institute of Technology, N-7034, Trondheim, Norway

Received 25 August 1993, accepted for publication 24 September 1993

Abstract. Ballistic electron transport in a Π-shaped quantum wire is investigated. The device conductance and bound-state energies are calculated on the basis of the tight-binding formalism. It is shown that the transmission coefficient as a function of the distance between the source and drain wires of the Π structure d is represented by a quasi-periodic sequence of unity transmission separated by valleys of nearly zero transmission. This is the case in the energy region of the stop-band behaviour of a right-angle-bend waveguide of the same width w. The bound-state spectrum of the Π and double-bend structures is studied in the entire region of variations of the parameter $\alpha = d/w$. In the double bend, the lowest bound-state energy ΔE_b is shown to be a non-monotonic function of α, which is zero at $\alpha = -1$ (the limiting case of a straight wire), reaches its maximum $\Delta E_b^{max} \approx 0.15$ (in units of the energy of the propagation threshold E_{th}) at $\alpha \approx -0.3$, and then tends to the asymptotic value ≈ 0.07, which corresponds to the bound-state energy in a right-angle-bend waveguide. Special emphasis is paid to the possibility of experimental identification of quantum interference effects.

Advances in modern nanotechnology, in particular the development of submicron lithography and the split-gate technique, have made possible the fabrication of lateral structures with different geometries, where electrons undergo two-dimensional (2D) motion. The lateral confinement of the high-mobility 2D electron gas at the semiconductor interface in heterostructures like $Al_xGa_{1-x}As/GaAs$ provides the conditions for ballistic transport, i.e. the electron free path is larger than the characteristic size of the device. Furthermore, the latter is comparable to or larger than the de Broglie wavelength. Under such conditions, the conducting properties of the device are completely determined by both quantum size effects and quantum interference effects.

Electron ballistic transport in various 2D geometries that are of interest for device applications has been a subject of many experimental [1–5] and theoretical [6–18] studies. Despite significant progress in this field, there is a lack of one-to-one correspondence between theoretical predictions and experiment [5]. Here we point out that in a simple Π-shaped two-terminal structure (figure 1(a, b)) with the parameters modified by the gate voltage, quantum interference effects in the region of the fundamental mode propagation can be reliably identified. This possibility arises from the fact that a right-angle-bend waveguide is characterized by the resonant-reflection (stop-bend) point in its transmission spectrum. Because of this and the interference of electron waves in the shoulder that connects the source and drain wires in the Π structure (see figure 1(b)), the transmission coefficient in the region of the stop-band behaviour of the Π structure can be drastically changed by small variations in the distance d, providing the wire width w remains constant. The resulting changes should manifest themselves as repeated sharp peaks followed by nearly zero conductance.

The double-bend structure (figure 1(c)), which has already been realized experimentally [5], has a similar transmission spectrum and thus it possesses the same property. But in the latter case it is difficult to conceive of appropriate experimental conditions to produce the predicted effect. Therefore, we focus our attention primarily on electron propagation in Π-shaped waveguides. On the other hand, it is also of interest to consider the double-bend structure, and particularly to trace the dependence of the bound-state spectrum on variations of d from $d = -w$ to $d = \infty$. This dependence has previously been studied only in the region $0 \leqslant d \leqslant \infty$ in [15].

We begin with an explicit form of the basic equations for the model. These equations are very similar to those for the double-bend and single-bend structures also considered. To describe ballistic electron transport through the structures shown in figure 1, we use the one-particle Hamiltonian in the tight-binding representation

0268-1242/93/122115+06$07.50

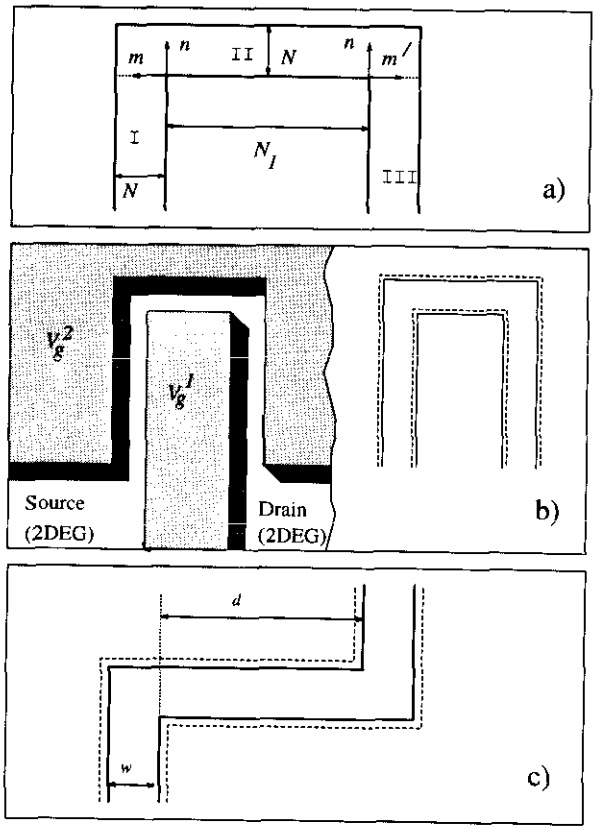

Figure 1. Schematic diagrams of the Π-shaped (*a*) and double-bend (*c*) waveguides (the correspondence between the parameters in the discrete and continuous models is: $a(N+1) = w$, $a(N_1 - 1) = d$, where a is the lattice constant). (*b*) Split-gate configuration of the Π structure. Shaded regions correspond to areas depleted by the applied gate voltages V_g^1 and V_g^2. 2DEG denotes the two-dimensional electron gas in the source and drain reservoirs. Broken lines indicate the modified channel which has the same width but different shoulder length d.

$$H = \sum_{m,n} \left(\varepsilon a^+_{m,n} a_{m,n} + L a^+_{m,n} \sum_{m',n'} a_{m',n'} \right) \qquad (1)$$

where the summation over m and n covers all sites of a regular plane lattice that forms the structure of the given shape confined by the hard-wall potential. The summation over m' and n' is performed over the lattice sites nearest to the site (m, n); $a^+_{m,n}$ $(a_{m,n})$ is the electron creation (annihilation) operator at the site (m, n), ε is the electron site energy and L is the energy of the resonant electron transfer between the neighbouring lattice sites. Note that, if passing to the continuum limit (see below), solutions of the Schrödinger equation with the Hamiltonian (1) are completely equivalent to the description in the framework of the continuous model of the structure [17] (for a more detailed formulation of the model see [18]).

The solution of the time-independent Schrödinger equation

$$H\Psi = E\Psi \qquad (2)$$

which describes the electron motion in the Π structure is given by

$$\Psi^\gamma = \sum_{m,n} A^\gamma_{m,n} a^+_{m,n} |0\rangle \qquad (3)$$

where the label $\gamma = \mathrm{I}, \mathrm{II}, \mathrm{III}$ refers to the regions shown in figure 1(*a*). Further specification of the problem is determined by the form of the amplitudes

$$A^{\mathrm{I}}_{m,n} = \sqrt{\frac{2}{N+1}} \sum_{j=1}^{N} \sin(\xi_j m) \times (\delta_{jj_0} e^{ik_j n} + r_{k_j} e^{-ik_j n}) \qquad \xi_j = \frac{\pi j}{N+1} \qquad (4)$$

and

$$A^{\mathrm{III}}_{m,n} = \sqrt{\frac{2}{N+1}} \sum_{j=1}^{N} \sin(\xi_j m') t_{k_j} e^{-ik_j n} \qquad (5)$$

which suggests that there are incident and reflected electron waves in the source lead I and only transmitted electron waves in the drain lead III. For simplicity, both leads are supposed to be infinite. The choice of the site coordinates used in equations (4) and (5) is shown by arrows in figure 1(*a*) In this case, $1 \leqslant m, m' \leqslant N$, $n \leqslant 0$ (for the inner region II $1 \leqslant n \leqslant N$, $-(N_1 - 1) \leqslant m \leqslant 0$), N is the wire width and N_1 is the distance between the leads I and III expressed as the number of lattice sites. For the double-bend structure shown in figure 1(*c*), the exponent in equation (5) should be replaced by $\exp[ik_j(n - N - 1)]$ with $n \geqslant N + 1$. The energy of incident electrons is $E = \varepsilon + 2L\{\cos k_0 + \cos[\pi j_0/(N+1)]\}$; the wavevectors k_j in equations (3) and (4) for both propagating $j \leqslant j_0$ and evanescent $j \geqslant j_0$ modes obey the energy conservation law:

$$\cos k_{j_0} + \cos[\pi j_0/(N+1)] = \cos k_j + \cos[\pi j/(N+1)].$$

Using equations (3)–(5) in equation (2), one can easily exclude the inner part of the wavefunction by means of the Green function technique, as was demonstrated previously for similar structures [17]. Note that, as distinct from the technique used by Sols *et al* [8] where the treatment of the wire discontinuities demands considerable computational effort, we arrive at explicit equations for quantities of direct physical interest—the amplitudes of reflected and transmitted waves. In this sense our approach is equivalent to the standard matching procedure with a single but obviously important advantage: the divergency known to be inherent in the continuous model is removed.

The resulting equation is

$$Z_j x^\pm_j = -2i \sin k_j \delta_{j,j_0} + \sum_{j'=1}^{N} Q^\pm_{jj'} x^\pm_{j'} \qquad (6)$$

where

$$x^\pm_j = \delta_{j,j_0} + r_{k_j} \pm (-1)^{j+1} t_{k_j} \qquad (7)$$

$$Z_j = \frac{\sin k_j \exp[-i(N+1)k_j]}{\sin[(N+1)k_j]} \qquad (8)$$

and

$$Q^\pm_{jj'} = \frac{\sin\xi_j \sin\xi_{j'}}{(N+1)^2} \sum_{j''=1}^{N} \frac{\sin^2\xi_{j''} \sin[(N+1)k_{j''}]}{\sin(k_{j''}) \sin[(2N+N_1+1)k_{j''}]} \times \frac{\sin[(N+N_1)k_{j''}] \pm f_{j''} \sin[(N+1)k_{j''}]}{(\cos k_j - \cos\xi_{j''})(\cos k_{j''} - \cos\xi_{j'})}. \qquad (9)$$

Passing to the continuum limit, $N \to \infty$, $w = (N+1)a = \text{const}$, $(N_1 - 1)/(N+1) = d/w = \text{const}$, it is convenient to set $\varepsilon = -4L$ and $m^* = -\hbar^2/2La^2$, where $L < 0$ for the positive effective mass and a is the lattice constant. Then equations (6) and (7) can be transformed to

$$Z_j^c x_j^{\pm} = -2i\, q_j \delta_{j,J_0} + \sum_{j'=1}^{\infty} Q_{jj'}^{c\pm} x_{j'}^{\pm} \tag{10}$$

where

$$Z_j^c = \frac{q_j \exp(-i\pi q_j)}{\sin(\pi q_j)}$$

$$Q_{jj'}^{c\pm} = \frac{4}{\pi^2} jj' \sum_{j''=1}^{\infty} \frac{j''^2 \sin(\pi q_{j''})}{q_{j''} \sin[(2+\alpha)\pi q_{j''}]} \times \frac{\sin[(1+\alpha)\pi q_{j''}] \pm f_{j''} \sin \pi q_{j''}}{(q_j^2 - j''^2)(q_{j''}^2 - j'^2)}. \tag{11}$$

In the above equations $\alpha = d/w$ and the longitudional wavevectors q_j are expressed in units of the propagation-threshold wavevector $k_{th} = \pi/w$ so that $E/E_{th} = q_{j_0}^2 + j_0^2$, $q_j = (q_{j_0}^2 + j_0^2 - j^2)^{1/2}$ and $E_{th} = \hbar^2 k_{th}^2/2m^*$; $f_j = 1$ for the Π structure and $f_j = (-1)^{j+1}$ for the double-bend structure.

The equations derived above have the form

$$\sum_{j'=1}^{N} S_{jj'}^{\pm} x_{j'}^{\pm} = F_j \tag{12}$$

where $S_{jj'}^{\pm} = Z_{j'}\delta_{jj'} - Q_{jj'}^{\pm} = S_{j'j}^{\pm}$, which can be regarded as canonical for two-terminal structures with any kind of square-corner discontinuities but with input and output leads of the same width. In particular, the only change that should be made in equation (12) to describe a single right-angle bend is that $Q_{jj'}^{\pm}$ (or $Q_{jj'}^{c\pm}$) should be replaced by $\pm G_{jj'}$ (or $\pm G_{jj'}^c$) where

$$G_{jj'} = \frac{1}{N+1} \frac{\sin\xi_j \sin\xi_{j'}}{\cos k_j - \cos\xi_{j'}} \qquad G_{jj'}^c = \frac{2}{\pi} \frac{jj'}{j^2 - q_{j'}^2}. \tag{13}$$

Some of the transmission properties of the structures discussed here can be predicted without solving the equations for the S matrix. For instance, let us consider the case of the minimal distance between leads I and III ($N_1 = 1$ for the discrete model and $d = 0$ for the continuous one) when the Π structure transforms into a semi-infinite wire of width $2w$ with a cut in its middle. In this structure the amplitudes of the reflected and transmitted waves are equal for all modes except that corresponding to the incident wave mode. This follows directly from equations (6) and (10), since $Q_{jj'}^{-} = 0$ for $N_1 = 1$ and $Q_{jj'}^{c-} = 0$ for $d = 0$. The double-bend structure with $d = 0$ evidently does not possess such a property. Furthermore, it is easy to show that in accordance with equation (12) (see also the corresponding definitions of the coefficients in it) the equation $t_{k_1} = 0$ (equivalently $x_1^+ = x_1^-$) is real in the region of the first-subband energy. Therefore, one can expect the stop-band behaviour in the single-mode transmission. This quantum interference effect is a specific property of two-terminal systems and is illustrated below for the single-bend, double-bend and Π structures. It is not expected for systems with a larger number of terminals (wire intersections, etc) since, in general, the equation $t_{k_j} = 0$, as well as $r_{k_j} = 0$, is complex. An exception in this sense is the T-type intersection. Because of its symmetry, this structure can act like a two-terminal one, which has the resonance reflection slightly below the opening of the second-mode propagation [13].

In what follows we restrict ourselves to the energy region of the fundamental mode propagation. The quantities of interest to us here are the transmission coefficient $T = |t_{k_1}|^2$ and the device conductance at

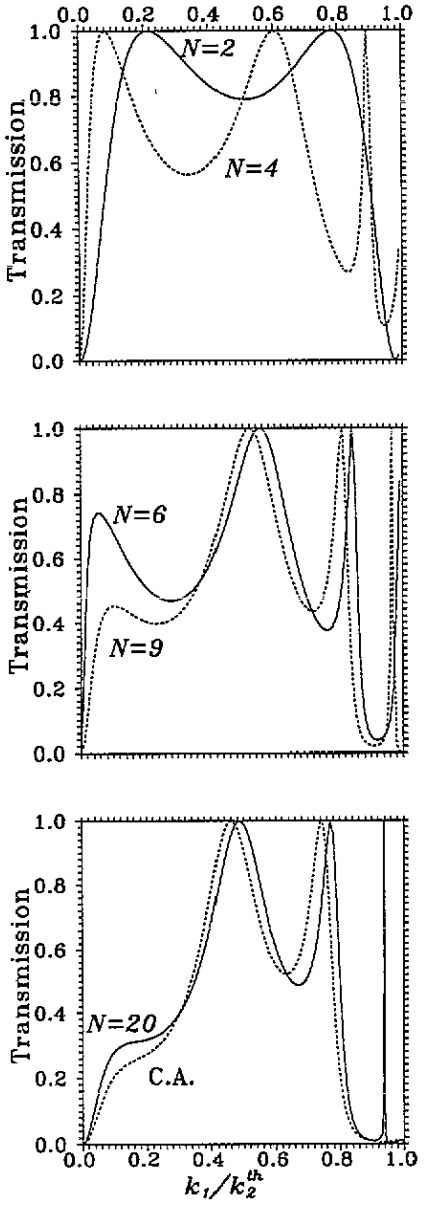

Figure 2. Dependence of the transmission coefficient T on electron wavenumber k_1/k_2^{th} in Π-structures with $d = w$ for different wire widths $w = (N+1)a$, $N = 2, 4, 6, 9, 20$; C.A. corresponds to the continuum limit (see text) and k_2^{th} is the threshold wavevector of the second-mode opening.

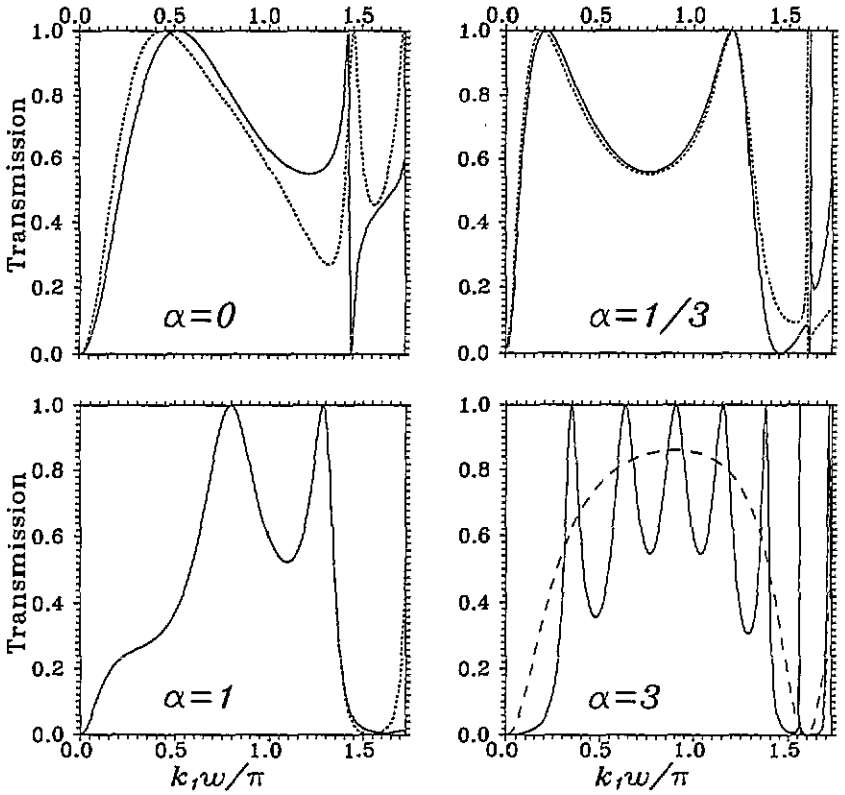

Figure 3. Transmission coefficient as a function of wavenumber (normalized to the propagation threshold wavevector π/w) for different ratios $d/w = \alpha$. Full and broken curves correspond to the Π- and double-bend structures respectively. The long-broken curve represents the transmission spectrum of a right-angle bend waveguide.

zero temperature and negligible bias voltage, $G = (2e^2/h)T(E_F)$ [19, 20], where E_F is the Fermi energy of the electron gas at zero bias.

First we note that the difference between the discrete and continuous models can be disregarded for wire widths $N \geqslant 20$. For narrower wires the discrete nature is important; see figure 2. Thus the continuous model is reliable for wire widths $\sim$ 10 nm or greater. This restriction is assumed to be obeyed in all the results presented below.

As expected, the transport properties of the Π and double-bend structures are appreciably different only for small values of the parameter $\alpha = d/w$; see figure 3. They are already practically identical when $\alpha = 1$. The curve that corresponds to $\alpha = 3$ is essentially the same as that calculated for the double-bend structure (the latter has been studied in detail by Weisshaar *et al* [5, 10]). It represents a single-bend transmission dependence (broken curve) with a typical interference pattern superimposed. The larger the value of α, the greater number of resonant peaks observable in the transmission coefficient. Every new peak arises near the threshold of second-mode propagation and then (with the further increase of α) shifts towards lower electron energies. Figure 4(*a*) shows the motion and shape transformations of new peaks in the transmission spectrum with increasing α. If the energy of electrons entering the Π-shaped device is fixed at or near the point of zero transmission, an increase (or decrease) of α will result in a quasi-periodic change in the transmission coefficient (figure 4(*b*)): areas of low transmission, including the point where $T = 0$, are separated by sharp peaks of the resonant transmission $T = 1$. The conductance of the Π structure is determined by the transmission coefficient (at zero temperature and negligible bias voltage), so to observe the predicted behaviour of the transmission it is necessary to increase, say, the lower negative gate voltage V_g^1 (figure 1(*b*)) and to decrease the upper gate voltage (or vice versa) in coordination, in order to keep the wire width constant while changing the distance d. This can be done in principle by using equal and opposite changes in gate voltage which vary d without affecting w to first order. A possible construction of a Π-shaped channel and of the necessary modifications (achieved if $\Delta V_g^1 = -\Delta V_g^2$) is shown in figure 1(*b*). Usually variations of the gate voltage result in a depletion area of the same extent in the longitudinal and lateral directions, i.e. the distance d changes by the same amount as the width of the wire w; see figure 1(*c*). Then the dependence of G on d or equivalently on w will be qualitatively different from that shown in figure 4(*b*). In the latter case the dependence $G(w)$ would have a very similar shape to the transmission spectrum shown in figure 3 for $\alpha = 3$, as was demonstrated by the calculations of Weisshaar *et al* [5, 10]. The complex structure of $G(w)$ with a number

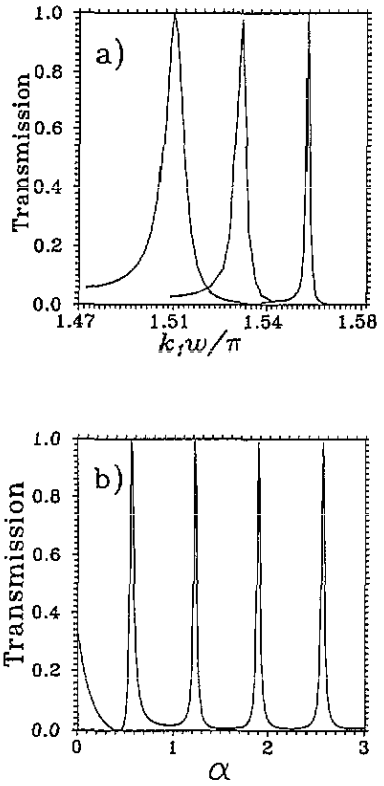

Figure 4. (*a*) Transmission coefficient $T(k)$ for different values of $\alpha = 3, 3.1, 3.2$ (from left to right). (*b*) Dependence of the transmission coefficient T on α for fixed $k_1 w/\pi = 1.5$.

of close resonant peaks makes the comparison with real experiment ambiguous. In this respect the clear-cut switch-type characteristic shown in figure 4(*b*) seems to be much easier for identification. We believe that the observation of such a dependence is quite possible and, if put into practice, will help elucidate quantum interference effects which, to our knowledge, have not been reliably identified in 2D electron waveguides.

In the energy region that is of most interest here (near the opening of the second mode) the simplified model of the Π-structure with infinite source and drain leads is supposed to reproduce sufficiently well the characteristic of the device shown in figure 1(*b*), providing that the length of the leads is greater than d. At the same time, it cannot be used to model the device conductivity near the threshold of electron propagation of a structure embedded in the split-gate configuration, which begins and ends in an effectively infinite 2D electron gas. An additional effect expected in this region is resonant tunnelling through the bound states that are known to reside near wire discontinuities [8, 9, 14–18]. The bound-state spectrum of the Π and double-bend structures is shown in figure 5 as a function of $\alpha = d/w$; $\alpha > -1$. For the case of $\alpha > 0$, the results presented are essentially the same as calculated previously [15]. But unlike the latter we also include the region $-1 < \alpha < 0$ for the double-bend structure.

It is remarkable that the difference in the bound-state energies of the Π and double-bend structures is small even when d tends to zero. When $d \to \infty$, the energy of the double-degenerate bound state coincides with that

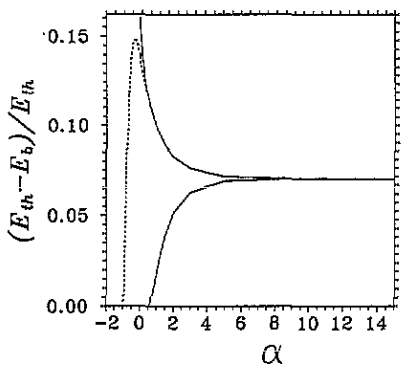

Figure 5. Bound-state energies versus α in the Π-structure (*full curves*) *and double-bend structure (broken curves).*

for a single bend, $\Delta E_b = (E_{th} - E_b)/E_{th} = 0.0696$ [9, 18]. A noticeable splitting of the even-parity (upper curve) and odd-parity (lower curve) bound states is observed at $\alpha < 6$. The odd-parity state disappears at $\alpha \approx 0.5$ for both structures. The splitting originates from the interaction (via the continuous spectrum of the waveguide) between the two states which are associated with the discrete levels in the vicinities of the structure bends. Obviously, since there is no direct interaction between the two bends, the bound-state splitting in 2D waveguides is a purely quantum mechanical effect, just like the existence of discrete levels in classically unbound systems [9].

As pointed out above, there exists only one bound state in the region $-1 \leqslant \alpha \leqslant 0.5$. The deepest discrete level corresponds to the double-bend structure with $\alpha \approx -0.3$ (not with $\alpha = 0$ as was presumably suggested in [15]). In this case $\Delta E^{max}_{b(db)} \approx 0.148$. When α tends to -1 (and the structure transforms into a straight wire) $\Delta E^{max}_{b(db)}$ falls to zero. The maximum departure of the bound state from the continuous spectrum in the Π structure (at $\alpha = 0$) is noticeably greater than in the double-bend structure, $\Delta E^{max}_{b(\Pi)} = 0.161$.

To conclude, equations for the S-matrix of electrons scattered in the Π, double- and single-bend structures have been presented for the first time in a simple explicit form. On this basis the bound-state spectrum and conductance of the degenerate Fermi gas in these structures have been calculated. It has been demonstrated that, as a result of the quantum interference in a Π-structure device, a quasi-periodic sequence of zero and sharp-spike conductance can be observed under varied gate voltages. The effect seems to be available for identification in a relevant experimental set-up.

References

[1] van Wees B J, van Houten H, Beenakker C W J, Williamson J G, Kouwenhoven L P, van der Marel D and Foxon C T 1988 *Phys. Rev. Lett.* **60** 848

[2] Wharam D A, Thornton T J, Newbury R, Pepper M, Ahmed H, Frost J E F, Hasko D G, Peacoc D C, Ritchie D A and Jones G A C 1988 *J. Phys. C: Solid State Phys.* **21** L209

[3] Brown R J, Kelly M J, Newbury R, Pepper M, Miller B, Ahmed H, Hasko D G, Peacock D C, Ritchie D A, Frost J E F and Jones G A C 1989 *Solid-State Electron.* **32** 1179

[4] Wieck A D and Ploog K 1990 *Appl. Phys. Lett.* **56** 928
[5] Wu J C, Wybourne M N, Yindeepol W, Weisshaar A and Goodnick S M 1991 *Appl. Phys. Lett.* **59** 102
[6] Levinson I V 1988 *Pis'ma v Zh. Exp. Teor. Fiz.* **48** 273 (1988 *JETP Lett.* **48** 301)
[7] Szafer A and Stone A D 1989 *Phys. Rev. Lett.* **62** 300
[8] Sols F, Macucci M, Ravaioli U and Hess K 1989 *Appl. Phys. Lett.* **54** 350; 1989 *J. Appl. Phys.* **66** 3892
[9] Schult R L, Ravenhall D G and Wyld H W 1989 *Phys. Rev.* B **39** 5476
[10] Weisshaar A, Lary J, Goodnick S and Tripathi V 1989 *Appl. Phys. Lett.* **55** 2114
[11] Kirczenov G 1989 1989 *Phys. Rev.* B **39** 10452
[12] Lent C S and Kirkner D J 1990 *Appl. Phys. Lett.* **67** 6353
[13] Baranger H U 1990 *Phys. Rev.* B **42** 11479
[14] Berggren F and Ji Zhen-Li 1991 *Phys. Rev.* B **43** 4760
[15] Wu H, Sprung D W L and Martorell J 1992 *Phys. Rev.* B **45** 11960
[16] Gaididei Yu B, Malysheva L I and Onipko A I 1992 *Phys. Status Solidi* b **172** 667
[17] Gaididei Yu B, Malysheva L I and Onipko A I 1992 *J. Phys.: Condens. Matter* **4** 7103
[18] Klimenko Yu A, Malysheva L I and Onipko A I 1993 *J. Phys.: Condens. Matter* **4** 5215
[19] Fisher D S and Lee P A 1981 *Phys. Rev.* B **23** 6851
[20] Landauer R 1981 *Phys. Lett.* **A85** 91